HHS Public Access

Author manuscript

Osteoarthritis Cartilage. Author manuscript; available in PMC 2017 November 22.

Published in final edited form as:

Osteoarthritis Cartilage. 2016 May ; 24(5): 921–931. doi:10.1016/j.joca.2015.12.009.

Unilateral anterior crossbite induces aberrant mineral deposition in degenerative temporomandibular cartilage in rats

M. Zhang[†,a], **H. Wang**[‡,a], **J. Zhang**[†,a], **H. Zhang**[†], **H. Yang**[†], **X. Wan**[†], **L. Jing**[†], **L. Lu**[†], **X. Liu**[†], **S. Yu**[†], **W. Chang**[§,‖], and **M. Wang**[†,*]

[†]State Key Laboratory of Military Stomatology, Department of Oral Anatomy and Physiology and TMD, School of Stomatology, Fourth Military Medical University, Xi'an, China

[‡]Department of Cardiology, Xijing Hospital, Fourth Military Medical University, Xi'an, China

[§]Endocrine Research Unit, University of California, San Francisco, Veterans Affairs Medical Center, San Francisco, USA

[‖]Department of Medicine, University of California San Francisco, USA

Abstract

Objective—To investigate whether mechanical stress induces mineral deposits that contribute to matrix degradation at the onset of osteoarthritis (OA) in temporomandibular joint (TMJ) cartilage.

Design—Female Sprague–Dawley rats were subjected to an unilateral anterior crossbite (UAC) procedure. Histology, electron microscopy, and energy dispersive spectrometer (EDS) were used to examine cartilage matrix structures and composition of mineral deposit in the affected TMJ cartilage. Protein and/or RNA expression of phenotypic markers and mineralization modulators and matrix degradation was analyzed by immunohistochemistry and/or real-time PCR. Synthetic basic calcium phosphate (BCP) and calcium pyrophosphate dehydrate (CPPD) crystals were used to stimulate ATDC5 cells for their impact on cell differentiation and gene expression.

Results—Fragmented and disorganized collagen fibers, expanded fibrous spaces, and enhancement of matrix vesicle production and mineral deposition were observed in matrices surrounding hypertrophic chondrocytes in cartilage as early as 2-weeks post-UAC and exacerbated with time. The mineral deposits in TMJ cartilage at 12- and 20-weeks post-UAC had Ca/P ratios of 1.42 and 1.44, which are similar to the ratios for BCP. The expression of mineralization inhibitors, NPP1, ANK, CD73, and Matrix gla protein (MGP) was decreased from 2 to 8 weeks

[*]Address correspondence and reprint requests to: M. Wang, Department of Oral Anatomy and Physiology and TMD, School of Stomatology, Fourth Military Medical University, Xi'an, 710032, China. mqwang@fmmu.edu.cn (M. Wang).
[a]Authors contributed equally to this work.

Author contributions: Conception and design of the study: Mian Zhang, Jing Zhang and Meiqing Wang.
Sample and data collection: Mian Zhang, Helin Wang, Hongyun Zhang, Hongxu Yang, Xianghong Wan and Lei Lu.
Statistical analysis: Jing Zhang and Lei Jing.
Data review and interpretation: Wenhan Chang.
Drafting of manuscript: Mian Zhang, Helin Wang and Meiqing Wang.
Critical revision of manuscript: Xiaodong Liu and Shibin Yu.
Approving final manuscript version: Mian Zhang, Helin Wang, Jing Zhang, Hongyun Zhang, Hongxu Yang, Xianghong Wan, Lei Jing, Lei, Lu, Xiaodong Liu, Shibin Yu, Wenhan Chang and Meiqing Wang.

Competing interests: The authors do not have any conflicts of interest to report.

Supplementary data: Supplementary data related to this article can be found at http://dx.doi.org/10.1016/j.joca.2015.12.009.

post-UAC, so were the chondrogenic markers, Col-2, Col-X and aggrecan. In contrast, the expression of tissue-nonspecific alkaline phosphatase (TNAP) and MMP13 was increased 4-weeks post-UAC. Treating ADTC5 cells with BCP crystals increased MMPs and ADAMTS5 expression, but reduced matrix production in a time-dependent manner.

Conclusion—UAC induces deposition of BCP-like minerals in osteoarthritic cartilage, which can stimulate matrix degradation by promoting the expression of cartilage-degrading enzymes to facilitate OA progression.

Keywords

Calcium-crystal; Temporomandibular joint (TMJ); Osteoarthritis (OA); CPPD; BCP

Introduction

Aberrant mineral deposition is one of hallmarks of OA cartilage[1–5]. Osteoarthritic patients having intra-articular calcium crystals show more severe and rapid progression of OA phenotype than those without apparent crystal deposition[6,7]. Basic calcium phosphate (BCP) and calcium pyrophosphate dehydrate (CPPD) are two major forms of calcium-containing crystals found in the affected cartilage, meniscus tissue, and/or synovial fluid in OA patients[8–10], with CPPD crystals associated with more inflammatory responses than the BCP crystals[1]. CPPD crystals are composed of rhomboidal or rod shape $Ca_2P_2O_7$2H_2O$ which has a Ca:P ratio of about 1, while BCP crystals are mainly composed of hydroxyapatite $Ca_{10}(PO_4)_6(OH)_2$, octacalcium phosphate $Ca_8(HPO_4)_2(PO_4)_4{\cdot}5H_2O$ and tricalcium phosphate $Ca_3(PO_4)_2$, which have molar Ca:P ratios of 1.67, 1.33 and 1.50 respectively[11–13], making them structurally and chemically distinguishable from CPPD crystals[14]. It is, however, unclear whether the above crystals are simply end-point products of cartilage degradation or they play active roles in altering chondrocytic differentiation and cartilage matrix degradation at the onset of OA.

Matrix gla protein (MGP), ANK (ANKH inorganic pyrophosphate transport regulator), nucleotide pyrophosphatase/phosphodiesterase-1 (NPP1) and CD73 are known for their anti-mineralization actions. MGP is found in the extracellular matrix of cartilage, bone, and arterial vessel walls[15,16]. It has been reported that MGP over-expression decreased mineralization *in vitro*[17], and deficient MGP expression impaired bone growth and induced ectopic mineralization in the arterial vessel walls in mice[18] . Stimulation of human osteoarthritic chondrocytes with shear stress reduced MGP mRNA expression, providing a mechanism for enhanced mineralization due to mechanical impact[19]. ANK is a multiple-pass trans-membrane protein that exports pyrophosphate (PPi), an inhibitor of mineral propagation, to the extracellular milieu[20]. Although robust ANK expression was reported in OA knee cartilage[21], a loss of ANK function led to intracellular entrapment of PPi and reductions in extracellular PPi (ePPi) content, thereby permitting ectopic mineralization to occur[20]. Like ANK, NPP1 also acts in concert to inhibit mineralization[22]. NPP1, encoded by *Ennp1* gene, is a member of nucleotide pyrophosphatase/phosphodiesterase family that catalyzes reactions to produce ePPi and AMP from extracellular nucleotide triphosphates[23]. Osteoblasts cultured from *Ennp1*-null mice showed a reduced ePPi level (up to 50%) and hypercalcification[24]. The serum levels of NPP1 are negatively associated with OA severity

and matrix mineralization. In cartilage of end-stage OA patients, NPP1 expression is downregulated[25]. CD73 regulates extracellular mineralization by converting AMP to adenosine and Pi. Adenosine inhibits tissue-nonspecific alkaline phosphatases (TNAP) activity, which is a promoter of mineralization by enhancing PPi degradation and Pi accumulation. CD73 deficiency leads to increased TNAP activity, therefore favoring mineralization[26].

Abnormal biomechanical impact is a key factor in the development of OA[27,28]. Aberrant dental occlusion in human can induce degeneration of temporomandibular joint (TMJ)[29–33]. Recently, we have developed a unilateral anterior crossbite (UAC) procedure that could induce OA-like changes in the TMJ cartilage of rats and mice[34–37]. These models mimic human conditions of malocclusion and allow studies on the progression of cartilage/bone changes following the mechanical defects. Herein, we employed imaging, histological, and molecular biology techniques to investigate whether there are early mineral deposits in the UAC-induced OA cartilage, what their chemical compositions are, and how their appearance is associated with the progression of osteoarthritic phenotypes in the affected cartilage. Furthermore, we studied the effects of the synthetic BCP and CPPD crystals on the expression of inflammatory factors, enzymes that degrade matrix proteins, and phenotypic markers in cultured chondrogenic ATDC5 cells. Our overall hypothesis is that UAC induces the deposition of mineral crystals at the onset of OA to promote the expression of inflammatory factors and matrix degrading enzymes and alter chondrocyte differentiation, together facilitating cartilage degeneration.

Materials and methods

UAC rat model

One hundred and sixty 6-week-old female Spraguee–Dawley rats (140–160 g) were provided by the Animal Center of the Fourth Military Medical University. All rats were housed in pathogen-free room and fed with sterilized food and redistilled water during the study according to the protocols approved by the Ethics Committee of the Fourth Military Medical University. The rats were randomized into 10 groups (16 rats per group) for two procedures (sham and UAC) and five time points (2, 4, 8, 12 and 20 weeks). Every four rats from each group were housed in a single cage (measuring 50 × 40 × 25 cm). Environmental conditions were kept at a temperature of 20 ± 2° C and humidity of 55% ± 5%, with good ventilation, under 4 W of light intensity per square meter for 12 h per day. Sterilized wood chips were used as bedding material and replaced every 2 days. Rats were monitored twice daily for their health status. All sections of this report are constructed according to the Animal Research Reporting in Vivo Experiments (ARRIVE) guidelines.

UAC and sham procedures were approved by the Ethics Committee of the Fourth Military Medical University and applied to the rats as we previously described[34,35]. Briefly, after each rat was anesthetized by a single intraperitoneal injection of 1% pentobarbital sodium (0.35 ml/100 g weight), a small metal tube (length = 2.5 mm, inside diameter = 3 mm) was bonded to the left maxillary incisor [Fig. 1(A)]. Another metal tube (length = 4.5 mm, inside diameter = 3.5 mm) was bonded to the left mandibular incisor. The end of the latter tube was bended to create a 135°-angle leaning toward labial side to create a cross-bite relationship

between the top and bottom incisors. Each operation was completed within 5 min and all efforts were made to minimize suffering. No detachment of the metal tube was found during the entire experimental period. Control rats were subjected to the same procedure but no metal tube was adhered.

UAC and age-matched control rats were sacrificed by single intraperitoneal injection of overdose pentobarbital sodium at week 2, 4, 8, 12 or 20 post-operation. No significant difference was noticed in the manifestation of OA phenotype between the right and left TMJ cartilage in the UAC group. For each control or UAC group, the 16 right TMJs were used for histochemical and immunohistochemical staining ($n = 4$), von Kossa staining ($n = 4$), energy dispersive spectrometer (EDS) analyses ($n = 4$) and TEM study ($n = 4$). Every 4 of the 16 left joints from each group at each time point were randomly pooled for RNA extraction and real-time PCR analyses ($n = 4$ RNA samples/group/time point). Procedures of histochemistry, immunohistochemistry, RNA extraction and real-time PCR were described in detail in Supplemental Materials and Methods.

von Kossa and histological staining

TMJs were fixed in 2.5% glutaraldehyde for 48 h, dehydrated in ethanol, and embedded in a mixture of methyl methacrylate and dibutyl phthalate. Sections (20 μm thickness) were made by a Leica SP1600 hard tissue-slicer, and stained by von Kossa reagents (Baoman Biotech, Shanghai, China, GMS80045).

Measurements of total and calcified cartilage thickness

Central sagittal sections of TMJ were subjected to hematoxylin and eosin [Fig. 1(B)] or von Kossa staining. The image of condylar cartilage was divided into three sections with equal width (anterior, middle and posterior). A region of interest (ROI) at the center of each section was boxed (width: 200 μm, height: cartilage thickness) and analyzed for the thickness of the cartilage and the proportion of calcified cartilage. The values from three ROIs was averaged and reported for each sample.

Transmission electron microscopy (TEM)

TMJs were isolated and fixed in 2.5% glutaraldehyde in a phosphate buffer (pH 7.2) for 24 h, decalcified in 10% EDTA for 1 month, post-fixed in 1% osmium tetroxide for 1 h, dehydrated in ethanol, immersed in propylene oxide, and embedded in Epon812. Ultrathin sections (40 nm thickness) were cut, stained with uranyl acetate and lead citrate, and examined under a transmission electron microscope (H-600, Hitachi, Japan).

Scanning electron microscopy (SEM) and energy dispersive spectrometer (EDS) analysis

Undecalcified TMJ condyles were fixed in 2.5% glutaraldehyde in a phosphate buffer (pH 7.2) for 24 h, embedded in a mixture of methyl methacrylate and dibutyl phthalate, sectioned (30 μm thickness), stained with silver glass, coated with gold, examined by a Philips XL 30 electron microscope at 30 kV and a 20° tilt angle and imaged using an image acquisition software. The EDS images were also obtained in the same instrument. For EDS analysis, the selections of ROI in cartilage were the same as those for measurements of total and calcified cartilage thickness.

In vitro cell culture and BCP or CPPD crystals stimulation

ADTC5 cells (Ruilu, Biotech, Shanghai, China) were cultured at a density of $5 \times 10^3/cm^2$ in DMEM/F12 medium (Hyclone) containing 10% fetal bovine serum (Hyclone). At 80% confluence, cells were treated with BCP or CPPD crystals (50 (μg/ml; Synthetic procedures of BCP and CPPD crystals were described in detail in Supplemental Materials and Methods.) for 4, 8 or 24 h before harvests for mRNA extraction. Experiments were repeated on three separate cultures.

Statistical analysis

All the data used was got from independent samples or observations. Values are presented as the mean and 95% confidence intervals (CI) (lower and upper limits). Statistical analysis was performed using SPSS software, version 11.0 (SPSS Inc, IL, USA). For analysis of stained images, the measurement procedures were performed in a blinded fashion by two independent observers (JZ and LJ) and the average value of the two measurements from the same sample was used for further statistical analysis. Before comparison of UAC to age-matched control groups, the normality of data distribution was tested by Shapiroee–Wilk test with 95% confidence and Levene's test was used to assess homogeneity of variance. The data of two compared groups were from the populations of Gaussian distribution and consistent with homogeneity of variance. The assumptions of parametric tests were fulfilled and the statistical significance between two groups was evaluated by Student's *t*-test. The statistical significance was defined as $P < 0.05$.

Results

All rats were healthy and not used for other experiments before. No significant body weight changes were noticed between control and UAC groups at the five sampling times.

Matrix degeneration and aberrant mineral deposition in UAC cartilage

As shown in Fig. 2(A), articular chondrocytes in TMJ condylar cartilage of control rats (Con) were arranged sequentially in the fibrous, proliferation, prehypertrophic, and hypertrophic layers from the superficial to deep zones. Proteoglycans, stained by Safranin O reagents, were rich in prehypertrophic and hypertrophic cartilage in control rats. In contrast, the chondrocyte arrangement began to disorganize at 2 weeks after the UAC operation and this defect worsened with time, leading to disrupted demarcation between proliferative and prehypertrophic layers as early as 4 weeks post-operation [Fig. 2(A), UAC]. The proteoglycan content in the UAC cartilage began to decrease as early as 2 weeks post-UAC and was nearly absent at 20 weeks post-UAC. The thickness of total cartilage and hypertrophic layer was significantly reduced beginning at 8 weeks post-UAC [Fig. 2(C), (D)]. There was, however, an increase in the thickness of the calcified zone [Fig. 2(B)] and thus an overall increase in the ratio of calcified zone over the entire hypertrophic layer in the UAC cartilage [Fig. 2(E)]. Along with these morphological changes, the protein expression by immunohistochemistry of Col-II [Fig. 3(A), (C)] and Col-X [Fig. 3(B), (D)] protein and the mRNA expression of Col-II, Col-X, and aggrecan by quantitative PCR [Fig. 3(E)–(G)] were both decreased in UAC vs control groups. Despite these OA-like morphological changes, no apparent inflammatory response was observed in all UAC-treated samples.

TEM (Fig. 4) showed that most hypertrophic chondrocytes in TMJ cartilage of the control groups were found in well-delimited lacunae [Fig. 4(A)–(E)] that were surrounded by the tightly-organized collagen fibers [Fig. 4(F)–(J)]. In UAC cartilage, however, collagen fibers were disorganized and fragmented with increasing inter-fibers spaces. These changes in matrix organization worsened with time after the UAC operation [Fig. 4(K)–(O)]. Mineral deposition was observed around the hypertrophic chondrocytes, beginning 2 weeks after the UAC procedure [Fig. 4(P)–(T), arrowheads]. Those peri-cellular minerals were contained in abundant matrix vesicles (with diameters ranging from 50 to 200 nm) [Fig. 4(U)–(Y), arrows] that were located in close proximity to the cell member of hypertrophic chondrocytes [Fig. 4(U)–(Y), dotted lines], supporting the cellular origin of the vesicles. This phenomenon was not observed around the cells in the superficial zones of the control and UAC cartilage. These mineralizing activities and electron-opaque matrix vesicles also became apparent in 12- and 20-weeks control groups [Fig. 4(D), (E), arrowhead], indicating some spontaneous aging-induced mineral deposition. However, the intensity of this spontaneous mineralization was much weaker than that in the UAC-treated cartilage [Fig. 4(P)–(T)]. TEM studies also showed that hypertrophic chondrocytes in 20-week UAC group displayed patches of condensed chromatin in their nuclei [Fig. 4(T), arrows], discontinuous nuclear membrane, structurally damaged organelles, and numerous intracellular vacuoles, indicating the onset of cell necrosis. All of these data indicated the ability of mechanical stimulus to induce cell death and the production of matrix vesicles, and cartilage mineralization in the deep zones of TMJ cartilage.

UAC down-regulated the expression of mineralization inhibitors in TMJ cartilage

To explore mechanisms that enhanced mineralization in the UAC cartilage, we performed immunohistochemistry and/or real-time PCR analyses to examine the expression of the molecules that are known to inhibit or promote mineral deposition. In control groups, cells expressing MGP — an inhibitor of mineralization — were mainly found in the hypertrophic zone [Fig. 5(A)]. Interestingly, increased MGP expression was found in the hypertrophic layer of 2- and 4-week UAC groups and extended into the pre-hypertrophic zone, which MGP is usually absent at the basal state [Fig. 5(A)], leading to increases in the numbers of MGP-positive cells at these two early time points [Fig. 5(B)]. However, the numbers of MGP-positive cells were significantly reduced in the UAC cartilage 8 weeks after the operation, indicating a biphasic response of MGP expression to the mechanical stress [Fig. 5(B)]. Consistent with these immunohistological changes, we observed biphasic changes in the *Mgp* in TMJ cartilage of UAC rat, which increased at 2 and 4 weeks post-operation and decreased 8 weeks after the operation when compared to age-matched controls [Fig. 5(C)]. In contrast, the expression of *CD73* and *Ank* was significantly reduced in TMJ cartilage of UAC group at all time points [Fig. 5(D), (F)]. The expression of *Npp1* was significantly reduced in the UAC cartilage, but only at 2 and 4 weeks post-operation when compared to their age-matched controls [Fig. 5(E)].

In contrast anti-mineralization molecules, the expression of *Tnap*, which hydrolyzes PPi into Pi to promote the formation of BCP crystals, was up-regulated in the UAC groups at 4, 8, and 12 weeks post-operation, and this effect waned at 20 weeks post-operation [Fig. 5(G)]. The expression of matrix metal-loproteinase, *Mmp13*, which cleaves type II collagen, was

also up-regulated in the UAC groups in the similar time-dependent manner as seen in the expression of *Tnap* [Fig. 5(H)]. These data suggested that mechanical stimuli induced by UAC might have caused aberrant mineral deposition in deep layer of cartilage by suppressing the chondrocytic expression of mineralized inhibitors and by enhancing the expression of enzymes that facilitate mineralization.

Nature of BCP crystals deposition and its stimulated responses in cultured ATDC5 cells

We next compared the chemical compositions of the minerals deposited in TMJ cartilage of UAC vs Con rats using EDS technology. We confirmed an increase in calcium (Ca) and phosphorus (P) content in UAC cartilage [Fig. 6(A), (B)] vs their age-matched controls, beginning at 2 weeks post-operation. To study the chemical compositions of the mineral deposits before their propagation, we looked for single isolated crystal nodules. By SEM, we found those structures in only one of four joints from 12- and 20-week UAC group and none from the control groups. These crystal nodules were rich in calcium and phosphorus, but low in carbon content [Fig. 6(C)] and had averaged Ca/P ratio of 1.42 (ranging from 1.38 to 1.48) in 12-week and 1.44 (range from 1.39 to 1.49) in 20-week UAC groups [Fig. 6(D)]. These ratios are in the range characteristics of octacalcium phosphate (Ca/P = 1.33) and tricalcium phosphate (Ca/P = 1.50), two biological forms of BCP crystals.

To test whether calcium-containing crystals impact on chondrocyte functions, we exposed ATDC5 cells to two synthetic crystals (BCP or CPPD). We found that CPPD crystals (50 μg/ml) stimulated *Tnf-α* and *Il-1β* expression 4 and 8 h after the treatment, but this effect was absent after 24 h of treatment [Fig. 7(A), (B)]. CPPD crystals also increased the levels of *Adamts5, Mmp3, Mmp9* and *Mmp13* expression at all three time-points [Fig. 7(C)–(F)]. In contrast, BCP crystals (50 μg/ml) transiently stimulated *Tnf-α* expression only at 10- and 30-min (data not shown) time points and down regulated it at later time-points [Fig. 7(J)]. The same treatment of BCP increased *Il-1β* expression at the 4-h time point but reduced it at 8- and 24-h time-points when compared to controls [Fig. 7(K)]. The expression of *Adamts5, Mmp3* and *Mmp9* was increased at all three time-points, while Mmp13 level was only elevated after 24 h of treatment [Fig. 7(L)–(O)]. The expression chondrocytic markers — *Col-II, Col-X* and *aggrecan* — was decreased at all three time-points after treatments with CPPD [Fig. 7(G)–(I)] or BCP [Fig. 7(P)–(R)] crystals.

Discussion

Our studies support the idea that mechanical stimuli by UAC can enhance mineral accumulation of BCP-like minerals in the cartilage matrix in deep layers of TMJ condyle and this aberrant mineralization may contribute, at least in part, to the altered chondrocyte differentiation and the thinning of articular cartilage by promoting matrix degradation likely through the increased expression of matrix-degrading enzymes, as well as the expansion of the calcified cartilage (Fig. 8).

Although, the detailed mechanism(s) underlying the effects of UAC on mineral deposition remain to be explored, we observed the ability of this mechanical stimulus to increase the deposition of matrix vesicles and their mineralization around the affected chondrocytes, suggesting that abnormal mechanical impact may physically promote the budding and

deposition of matrix vesicles to serve as mineral nucleation sites[38,39]. Alternatively, those matrix vesicles may be by-products of UAC-induced cell necrosis as indicated by the condensed chromatin, discontinuous nuclear membrane, and damaged organelles in chondrocytes in the UAC-treated cartilage. After its seeding, the growth of BCP minerals is governed by local concentrations of substrates ($Ca^{2þ}$ and Pi), promoters (such as TNAP), and/or inhibitors (such as PPi). Our data suggested that UAC suppressed the expression of NPP1 and ANK, whose functions are to synthesize and export PPi, respectively, to block BCP crystal growth[20,23]. On the other hand, UAC promoted the expression of TNAP, whose functions are to hydrolyze PPi into Pi to remove the inhibitory effects of PPi and increase local [Pi] at the same time. Besides, UAC could also promote mineralization by suppressing the expression of CD73, which is known to inhibit TNAP activity[26], and/or by suppressing the production of MGP that directly blocks the propagation of mineral[17]. Our time-course studies well defined the temporal sequence of the above mineralizing events. The early transient up-regulation of MGP in hypertrophic chondrocytes may represent a protective response of the cells to resist initial mineral deposition due to UAC. This may explain the relatively mild mineralization and fewer mineral vestiges at those time points. This protective effect waned beyond the 8-week time point likely due to the reduction in the number of MGP-positive chondrocytes as a result of the accumulated calcium deposits in the surrounding matrix. The above changes in MGP expression paralleled with a transient decrease in NPP1 expression within 4 weeks of UAC, and a more prolonged increase in TNAP expression from 4 to 12-weeks of UAC treatment. The latter two events together are expected to reduce [PPi] in the cartilage and increase [Pi], therefore enhancing formation of BCP, but not CPPD, crystals in the UAC-treated cartilage.

It is also hypothesized that relaxation of collagen fiber is required for mineral deposition[40]. In the growth plate, the crystal formation normally occurs in the deeper (or mineralizing) hyper-trophic zone where matrix undergoes rapid remodeling by the increasing MMP activities in the terminally differentiated chondrocytes[41]. In contrast, in healthy articular cartilage, terminal differentiation of chondrocyte progress very slowly and this prevents rapid and extensive mineralization, therefore restricting mineral deposition to the deepest zone of the cartilage. However, in response to continuous UAC treatment in our animal models, the increased MMP13 expression in lieu of reduced expression of Col-II, Col-X and aggrecan matrix proteins could readily facilitate the mineral deposition[36] by degrading surrounding collagen fibers and by increasing inter-fibrous space[42,43]. Furthermore, our *in vitro* data that both BCP and CPPD crystals directly promoted the expression of different forms of MMPs and decreased the synthesis of matrix proteins, suggest that the initial mineral deposition in deep zone of the insulted cartilage may feed forward to enhance local MMPs' activity to facilitate calcification in the cartilage. This notion is in line with the time-course data, which showed that the UAC-induced mineralization occurred before cartilage thinning, but in parallel to the increased *Mmp*-13 expression.

Our histology did not show significant inflammatory responses in UAC-treated joints, despite the increased BCP-like deposition. Consistent to this *in vivo* observation, we observed only transient and marginal effects of BCP on *IL-1β* and *Tnf-α* expression in cultured ATDC5 cells when compared to the more robust effects of CPPD on these genes at the same concentration. These data support the idea that BCP crystals may induce less

inflammatory responses than CPPD crystals as indicated by other studies[1, 44] . It will be interesting to associate the types of minerals with pathological presentation of cartilage in different OA patients. It is unclear how the signals of BCP crystal were received by the chondrocytes and coupled to cellular functions. Even though some toll-like receptors may be involved in transmitting the stimulation of calcium-containing crystals into cells[45], the exact receptors that bind and respond to calcium-containing crystals remain to be defined. It is, therefore, difficult to develop loss-of-function strategies, like siRNA, to effectively block the stimulant signals of calcium-containing crystals and study its down-stream effectors.

Mineral deposition was detected by μCT technology in ≈65% of patients attaining temporomandibular joint disorders (TMD) as indicated by structural changes of their condyles. Studies by Fu *et al.*[46] showed that mineral deposition in cartilage matrix may be a biomarker for aberrant endochondral ossification that lead to the formation of osteophyma and sclerosis at chondro-osteo junctions. As our study clearly demonstrates that early mineral deposition in TMJ cartilage was due to malocclusion. Diagnostic and therapeutic values of those mineral deposits in biomechanically induced OA cartilage could be significant and warrant further investigations.

In conclusion, our findings suggest that UAC-derived mechanical stress induces aberrant mineral deposition at the onset of OA, which increases the thickness of calcified cartilage by promoting deep zone mineralization of cartilage but decreases the thickness of the cartilage by producing catabolic and differential signals at the insulted sites.

Supplementary Material

Refer to Web version on PubMed Central for supplementary material.

Acknowledgments

Funding sources: This work was supported by the National Natural Science Foundation of China for Meiqing Wang (No. 81530033) and Jing Zhang (No. 81500896).

We gratefully acknowledge Zhaohua Ji for assistance in statistical analysis and Shujing Cai for assistance in histology procedure.

References

1. Rosenthal AK. Calcium crystal deposition and osteoarthritis. Rheum Dis Clin North Am. 2006; 32:401–12. [PubMed: 16716886]
2. Ea HK, Lioté F. Advances in understanding calcium-containing crystal disease. Curr Opin Rheumatol. 2009; 21:150–7. [PubMed: 19339926]
3. MacMullan P, McMahon G, McCarthy G. Detection of basic calcium phosphate crystals in osteoarthritis. Joint Bone Spine. 2011; 78:358–63. [PubMed: 21273110]
4. Ferrone C, Andracco R, Cimmino MA. Calcium pyrophosphate deposition disease: clinical manifestations. Reumatismo. 2012; 63:246–52. [PubMed: 22303531]
5. Tsui FW. Genetics and mechanisms of crystal deposition in calcium pyrophosphate deposition disease. Curr Rheumatol Rep. 2012; 14:155–60. [PubMed: 22198832]
6. Gordon GV, Villanueva T, Schumacher HR, Gohel V. Autopsy study correlating degree of osteoarthritis, synovitis and evidence of articular calcification. J Rheumatol. 1984; 11:681–6. [PubMed: 6096542]

7. Nalbant S, Martinez JA, Kitumnuaypong T, Clayburne G, Sieck M, Schumacher HR Jr. Synovial fluid features and their relations to osteoarthritis severity: new findings from sequential studies. Osteoarthritis Cartilage. 2003; 11:50–4. [PubMed: 12505487]
8. Derfus BA, Kurian JB, Butler JJ, Daft LJ, Carrera GF, Ryan LM, et al. The high prevalence of pathologic calcium crystals in preoperative knees. J Rheumatol. 2002; 29:570–4. [PubMed: 11908575]
9. Abreu M, Johnson K, Chung CB, De Lima JE Jr, Trudell D, Terkeltaub R, et al. Calcification in calcium pyrophosphate dihydrate (CPPD) crystalline deposits in the knee: anatomic, radiographic, MR imaging, and histologic study in cadavers. Skelet Radiol. 2004; 33:392–8.
10. Wu CW, Terkeltaub R, Kalunian KC. Calcium-containing crystals and osteoarthritis: implications for the clinician. Curr Rheumatol Rep. 2005; 7:213–9. [PubMed: 15918998]
11. Halverson PB, McCarty DJ. Patterns of radiographic abnormalities associated with basic calcium phosphate and calcium pyrophosphate dihydrate crystal deposition in the knee. Ann Rheum Dis. 1986; 45:603–5. [PubMed: 3017246]
12. Halverson PB, Cheung HS, Johnson R, Struve J. Simultaneous occurrence of calcium pyrophosphate dihydrate and basic calcium phosphate (hydroxyapatite) crystals in a knee. Clin Orthop Relat Res. 1990; 257:162–5.
13. McCarty DJ, Lehr JR, Halverson PB. Crystal populations in human synovial fluid. Identification of apatite, octacalcium phosphate, and tricalcium phosphate. Arthritis Rheum. 1983; 26:1220–4. [PubMed: 6626280]
14. Fuerst M, Lammers L, Schäfer F, Niggemeyer O, Steinhagen J, Lohmann CH, et al. Investigation of calcium crystals in OA knees. Rheumatol Int. 2010; 30:623–31. [PubMed: 19639325]
15. Hale JE, Fraser JD, Price PA. The identification of matrix Gla protein in cartilage. J Biol Chem. 1988; 263:5820–4. [PubMed: 3258600]
16. Canfield AE, Doherty MJ, Kelly V, Newman B, Farrington C, Grant ME, et al. Matrix Gla protein is differentially expressed during the deposition of a calcified matrix by vascular pericytes. FEBS Lett. 2000; 487:267–71. [PubMed: 11150522]
17. Newman B, Gigout LI, Sudre L, Grant ME, Wallis GA. Coordinated expression of matrix Gla protein is required during endochondral ossification for chondrocyte survival. J Cell Biol. 2001; 154:659–66. [PubMed: 11489922]
18. Luo G, Ducy P, McKee MD, Pinero GJ, Loyer E, Behringer RR, et al. Spontaneous calcification of arteries and cartilage in mice lacking matrix GLA protein. Nature. 1997; 386:78–81. [PubMed: 9052783]
19. Lee MS, Sun MT, Pang ST, Ueng SW, Chen SC, Hwang TL, et al. Evaluation of differentially expressed genes by shear stress in human osteoarthritic chondrocytes in vitro. Chang Gung Med J. 2009; 32:42–50. [PubMed: 19292938]
20. Ho AM, Johnson MD, Kingsley DM. Role of the mouse ank gene in control of tissue calcification and arthritis. Science. 2000; 289:265–70. [PubMed: 10894769]
21. Johnson K, Terkeltaub R. Upregulated ank expression in osteoarthritis can promote both chondrocyte MMP-13 expression and calcification via chondrocyte extracellular PPi excess. Osteoarthritis Cartilage. 2004; 12:321–35. [PubMed: 15023384]
22. Harmey D, Hessle L, Narisawa S, Johnson KA, Terkeltaub R, Millán JL. Concerted regulation of inorganic pyrophosphate and osteopontin by akp2, enpp1, and ank: an integrated model of the pathogenesis of mineralization disorders. Am J Pathol. 2004; 164:1199–209. [PubMed: 15039209]
23. Richette P, Bardin T, Doherty M. An update on the epidemiology of calcium pyrophosphate dihydrate crystal deposition disease. Rheumatology. 2009; 48:711–5. [PubMed: 19398486]
24. Johnson K, Goding J, Van Etten D, Sali A, Hu SI, Farley D, et al. Linked deficiencies in extracellular PP(i) and osteopontin mediate pathologic calcification associated with defective PC-1 and ANK expression. J Bone Miner Res. 2003; 18:994–1004. [PubMed: 12817751]
25. Bertrand J, Nitschke Y, Fuerst M, Hermann S, Schäfers M, Sherwood J, et al. Decreased levels of nucleotide pyrophosphatase phosphodiesterase 1 are associated with cartilage calcification in osteoarthritis and trigger osteoarthritic changes in mice. Ann Rheum Dis. 2012; 71:1249–53. [PubMed: 22510396]

26. Eltzschig HK, Robson SC. NT5E mutations and arterial calcifications. N Engl J Med. 2011; 364:1577–8. [PubMed: 21506753]
27. Tragord BS, Gill NW, Silvernail JL, Teyhen DS, Allison SC. Joint mobilization forces and therapist reliability in subjects with knee osteoarthritis. J Man Manip Ther. 2013; 21:196–206. [PubMed: 24421632]
28. Røsland T, Gregersen LS, Eskehave TN, Kersting UG, Arendt-Nielsen L. Pain sensitization and degenerative changes are associated with aberrant plantar loading in patients with painful knee osteoarthritis. Scand J Rheumatol. 2015; 44:61–9. [PubMed: 25296895]
29. Patel DN, Manfredini D. Two commentaries on interventions for the management of temporomandibular joint osteoarthritis. Evid Based Dent. 2013; 14:5–7. [PubMed: 23579296]
30. de Souza RF, Lovato da Silva CH, Nasser M, Fedorowicz Z, Al-Muharraqi MA. Interventions for the management of temporomandibular joint osteoarthritis. Cochrane Database Syst Rev. 2012; 4:CD007261.
31. Wang M, Yao X, Yan C, Huang C, Zhang M, Zhang Y. A comparative study on the intercuspal occlusion among TMD patients, malocclusion patients and university students. Zhonghua Kou Qiang Yi Xue Za Zhi. 2002; 37:249–52. [PubMed: 12411168]
32. Wang MQ, Xue F, He JJ, Chen JH, Chen CS, Raustia A. Missing posterior teeth and risk of temporomandibular disorders. J Dent Res. 2009; 88:942–5. [PubMed: 19783804]
33. Wang XR, Zhang Y, Xing N, Xu YF, Wang MQ. Stable tooth contacts in intercuspal occlusion makes for utilities of the jaw elevators during maximal voluntary clenching. J Oral Rehabil. 2013; 40:319–28. [PubMed: 23480460]
34. Zhang J, Zhang HY, Zhang M, Qiu ZY, Wu YP, Callaway DA, et al. Connexin43 hemichannels mediate small molecule exchange between chondrocytes and matrix in biomechanically-stimulated temporomandibular joint cartilage. Osteoarthritis Cartilage. 2014; 22:822–30. [PubMed: 24704497]
35. Liu YD, Liao LF, Zhang HY, Lu L, Jiao K, Zhang M, et al. Reducing dietary loading decreases mouse temporomandibular joint degradation induced by anterior crossbite prosthesis. Osteoarthritis Cartilage. 2014; 22:302–12.
36. Wang YL, Zhang J, Zhang M, Lu L, Wang X, Guo M, et al. Cartilage degradation in temporomandibular joint induced by unilateral anterior crossbite prosthesis. Oral Dis. 2014; 20:301–6. [PubMed: 23614573]
37. Zhang M, Zhang J, Lu L, Qiu ZY, Zhang X, Yu SB, et al. Enhancement of chondrocyte autophagy is an early response in the degenerative cartilage of the temporomandibular joint to biomechanical dental stimulation. Apoptosis. 2013; 18:423–34. [PubMed: 23386193]
38. Kobayashi H, Saito T, Tanaka S. Mineralization of cartilage in growth plate. Clin Calcium. 2014; 24:177–84. [PubMed: 24473350]
39. Simão AM, Bolean M, Hoylaerts MF, Millan JL, Ciancaglini P. Effects of pH on the production of phosphate and pyrophosphate by matrix vesicles' biomimetics. Calcif Tissue Int. 2013; 93:222–32. [PubMed: 23942722]
40. Kirsch T, Wuthier RE. Stimulation of calcification of growth plate cartilage matrix vesicles by binding to type II and X collagens. J Biol Chem. 1994; 269:11462–9. [PubMed: 8157677]
41. Anderson HC. Matrix vesicles and calcification. Curr Rheumatol Rep. 2003; 5:222–6. [PubMed: 12744815]
42. Petursson F, Husa M, June R, Lotz M, Terkeltaub R, Liu-Bryan R. Linked decreases in liver kinase B1 and AMP-activated protein kinase activity modulate matrix catabolic responses to biomechanical injury in chondrocytes. Arthritis Res Ther. 2013; 15:R77. [PubMed: 23883619]
43. Chowdhury TT, Schulz RM, Rai SS, Thuemmler CB, Wuestneck N, Bader A, et al. Biomechanical modulation of collagen fragment-induced anabolic and catabolic activities in chondrocyte/agarose constructs. Arthritis Res Ther. 2010; 12:R82. [PubMed: 20462435]
44. Scanzello CR, Plaas A, Crow MK. Innate immune system activation in osteoarthritis: is osteoarthritis a chronic wound? Curr Opin Rheumatol. 2008; 20:565–72. [PubMed: 18698179]
45. Liu YZ, Jackson AP, Cosgrove SD. Contribution of calcium-containing crystals to cartilage degradation and synovial inflammation in osteoarthritis. Osteoarthritis Cartilage. 2009; 17:1333–40. [PubMed: 19447216]

46. Fu KY, Zhang WL, Liu DG, Chen HM, Ma XC. Cone beam computed tomography in the diagnosis of temporomandibular joint osteoarthrosis. Zhonghua Kou Qiang Yi Xue Za Zhi. 2007; 42:417–20. [PubMed: 17961362]

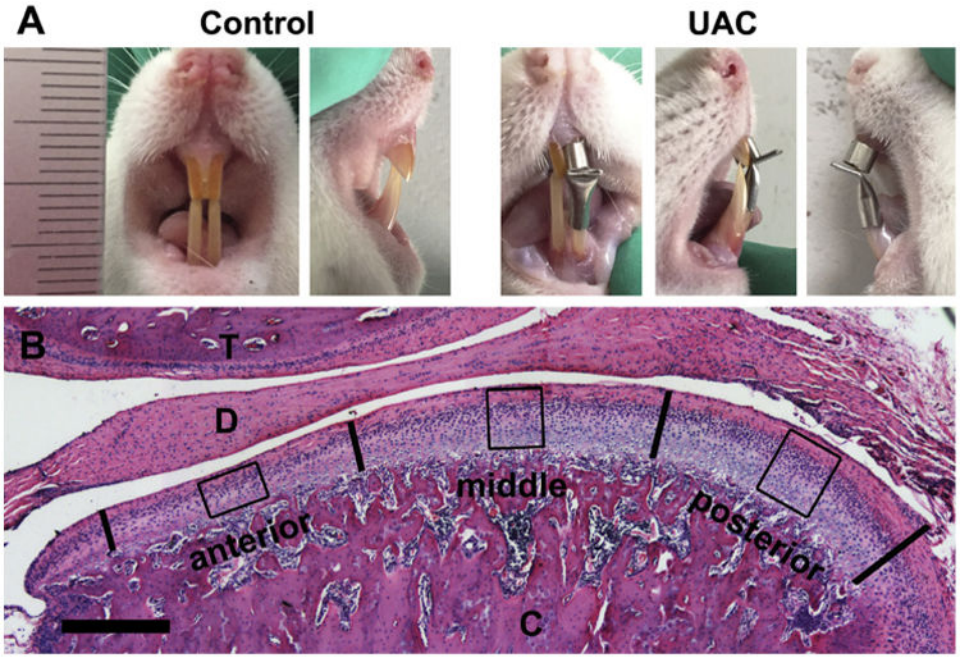

Fig. 1.

(A) The representative frontal and lateral views of anterior dental occlusion relationship in the control and UAC rats. (B) A typical central sagittal section of TMJ stained with hematoxylin and eosin. The bold vertical lines divide the articular cartilage of mandibular condyle into three equal sections (anterior, middle, and posterior). The boxes depict regions of interest in each section, which were included in quantitative analyses. T, temporal bone; D, articular disc; C, mandibular condyle.

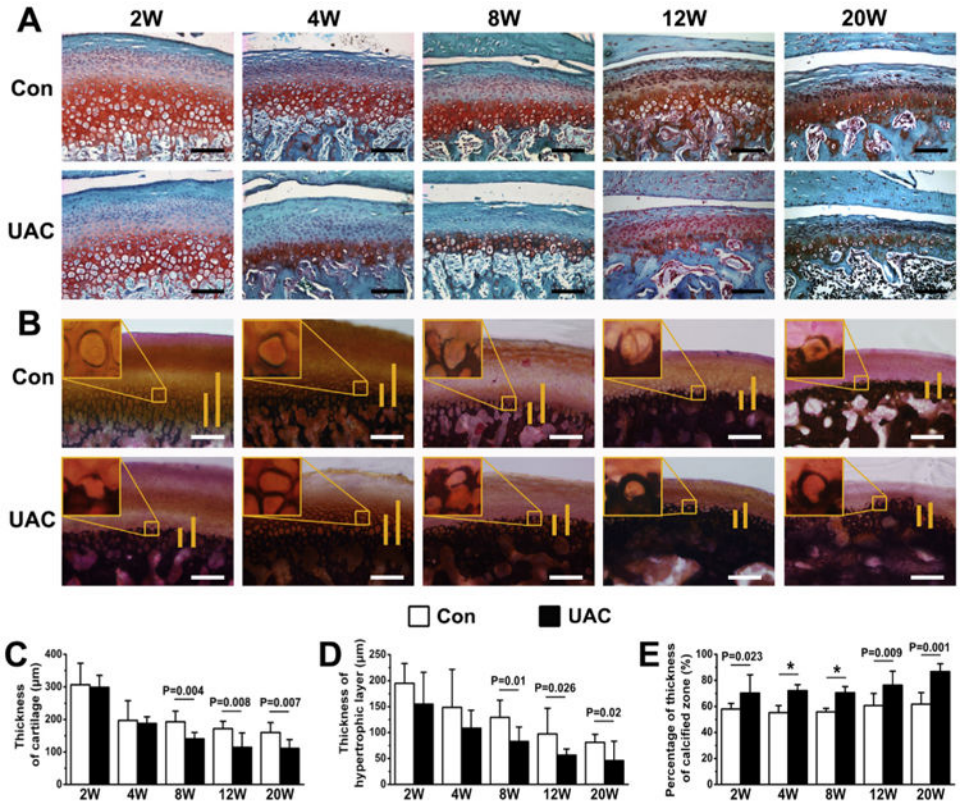

Fig. 2.

Histology staining of condylar cartilage from control and UAC rats at different time points (2, 4, 8, 12, and 20 weeks) after the operation. (A) Safranin O staining showed the irregularly arranged chondrocytes and reduced proteoglycan content in the cartilage of UAC vs control groups. (B) von Kossa staining showed expanded calcified zones in the UAC vs age-matched control cartilage. Long vertical bars depict total height of the hypertrophic cartilage. Short vertical bars indicate mineralized cartilage. Measurements of (C) total thickness, (D) hypertrophic layer thickness and (E) proportion of calcified cartilage in the mandibular condylar cartilage from UAC and control rats. $n = 4$ rats per group. Con, control group; UAC, UAC group; Bar = 100 μm. Values are represented as the mean with lower and upper limits of 95% CI. $*P < 0.0001$ or as specified.

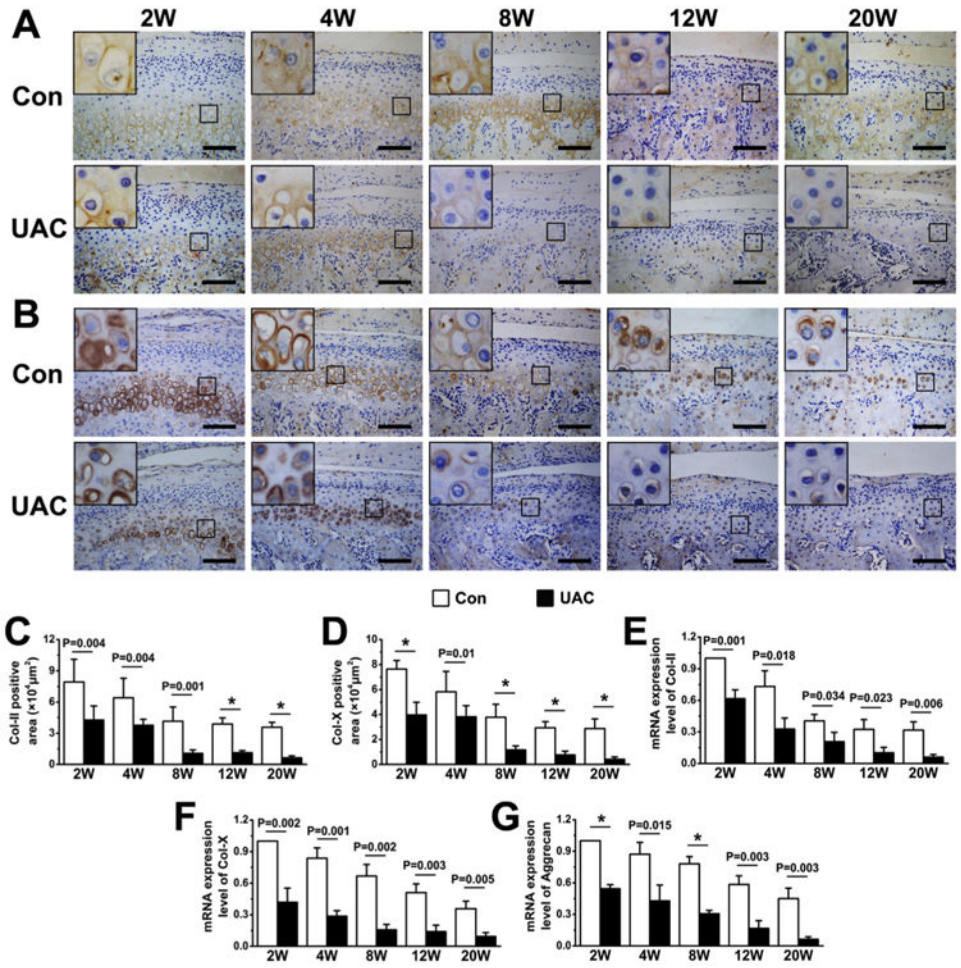

Fig. 3.

Immunohistochemical staining and quantitative real-time PCR analyses of condylar cartilage from control and UAC rats at different time points (2, 4, 8, 12, and 20 weeks) after the operation. (A–B) Immunohistochemical staining of Col-II (A, goat-anti-Col-II antibody) and Col-X (B, rabbit-anti-Col-X antibody) in control and UAC cartilage. (C–D) Determination of Col-II-positive areas (C) and Col-X-positive areas (D) in condylar cartilage from UAC and control rats. $n = 4$ rats per group. (E–G) Quantitative real-time PCR analyses for the expression of *Col-II* (E), *Col-X* (F) and *Aggrecan* (G). Analysis repeated for four times ($n = 4$). Values are represented as the mean with lower and upper limits of 95% CI. $*P < 0.0001$ or as specified.

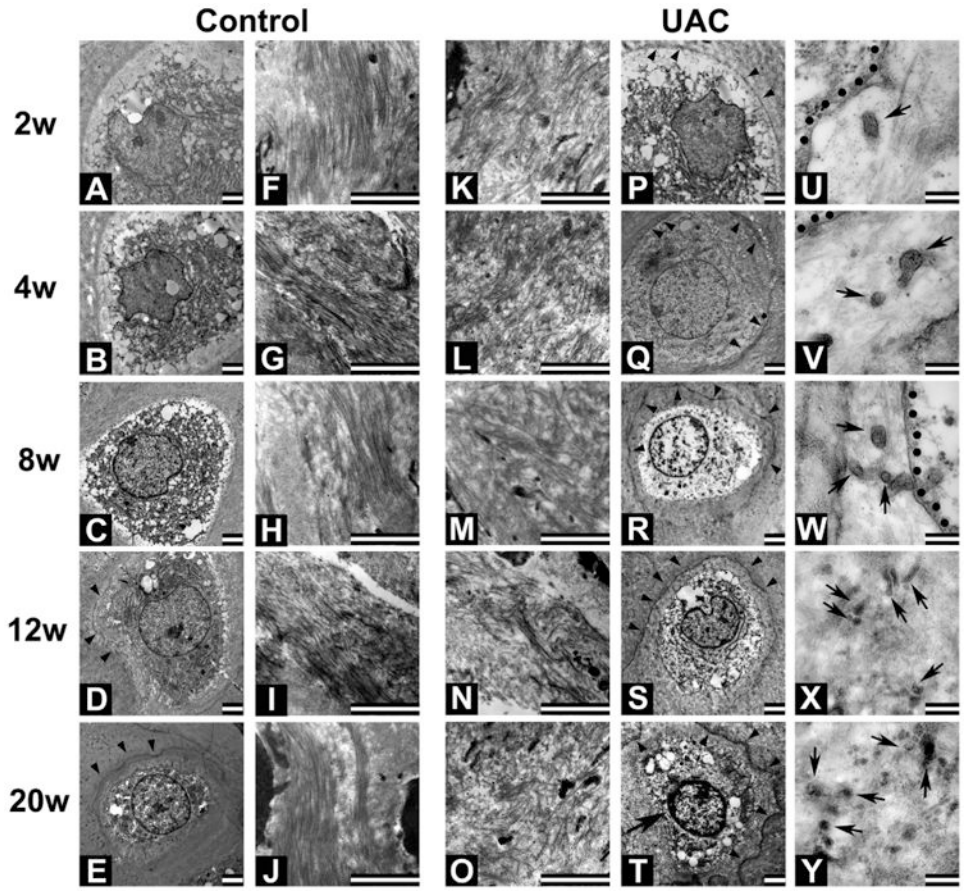

Fig. 4.

TEM images of hypertrophic chondrocytes and surrounding matrix in mandibular condylar cartilage from control (A–J) and UAC (K–Y) rats. Bar: 2 mm in A–T; 200 nm in U–Y. $n = 4$ rats per group. Collagen fibers in the matrices are tightly packed at all time points in control cartilage. Only slight vestige of mineralization (arrowhead) is observed in control cartilage beyond the 12-week time point (D and E). Fragmented collagen fibers and expanded interfiber spaces are obvious in UAC cartilage at all time points (K–O). In the latter cartilage, vestige of mineralization (PeT, arrowheads) is observed beginning 2 weeks after operation and aggravated with time. Intense mineral vestige is found in matrices surrounding the cell (T) displaying small patches of condensed chromatin (arrow), discontinuous membrane, structural damaged organelles and numerous intracellular vesicles. (U–Y) Enlarged images show vesicle-like structures in pericellular matrices surrounding hypertrophic chondrocytes in UAC-treated cartilage at all time points (dotted lines: membrane; arrows: vesicular structures adjacent to the cell membrane).

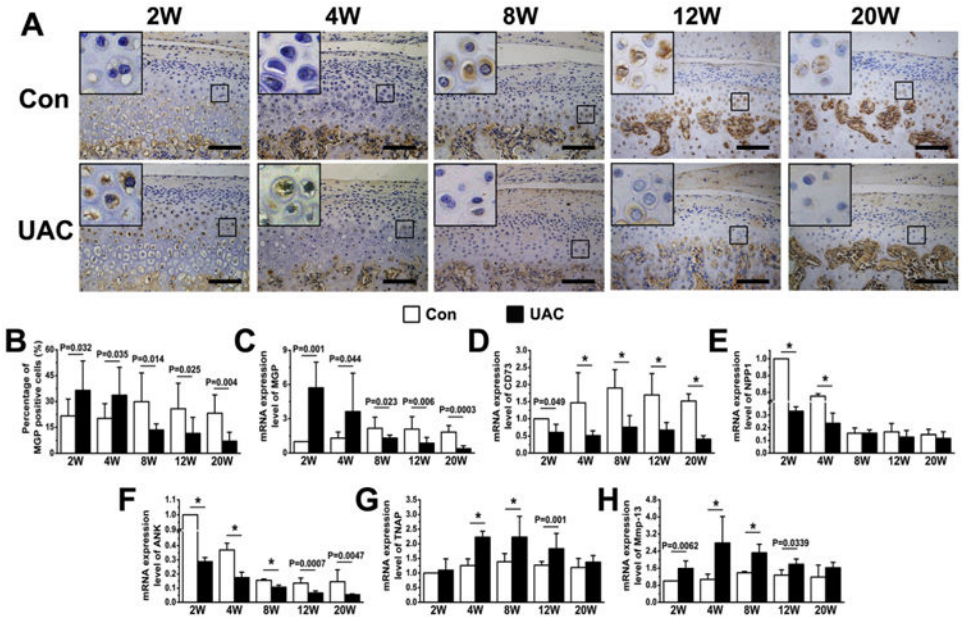

Fig. 5.

Immunohistochemical staining and quantitative real-time PCR analyses of condylar cartilage from control and UAC rats at different time points (2, 4, 8, 12, and 20 weeks) after the operation. (A) Immunohistochemical staining of MGP (rabbit-anti-MGP antibody) in control and UAC cartilage. (B) Numbers of MGP-positive cells in condylar cartilage from UAC and control rats. $n = 4$ rats per group. (CeH) Quantitative real-time PCR analyses for the expression of *Mgp* (C), *CD73* (D), *Npp1* (E), *Ank* (F), *Tnap* (G) and *Mmmp13* (H) in mandibular condyles of control and UAC rats. Analysis repeated for four times ($n = 4$). Values are represented as the mean with lower and upper limits of 95% CI. $*P < 0.0001$ or as specified.

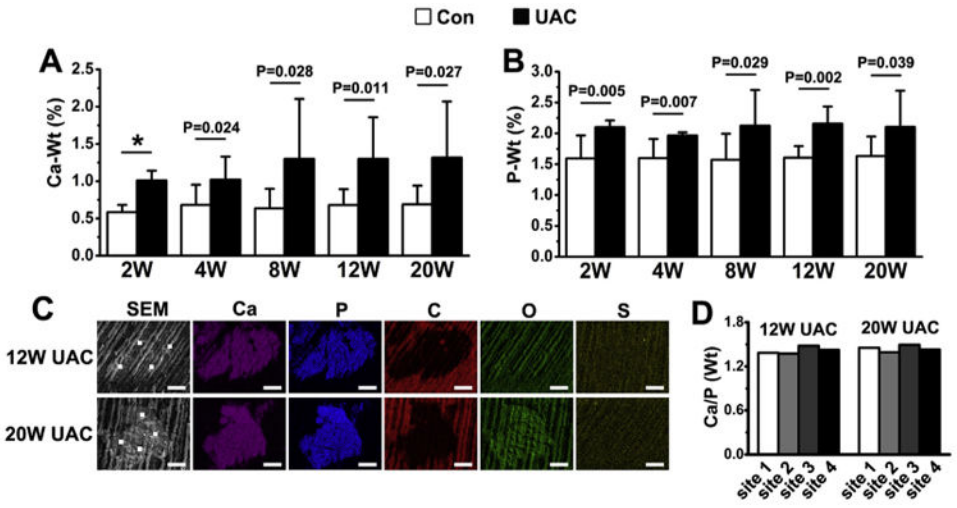

Fig. 6.

Ca (A) and P (B) contents in TMJ cartilage between UAC rats and their controls. $n = 4$ rats per group. Values are represented as the mean with lower and upper limits of 95% CI. $*P <$ 0.0001 or as specified. (C) The mineral nodules were visualized by SEM and their chemical compositions were quantified by EDS. Ca and P contents were enriched but C content was pinched in those nodules. White dots depict sites for EDS analyses; Ca, calcium; P, phosphorus; C, carbon; O, oxygen; S, sulphur. Bar = 5 μm. (D) Ratios of Ca to P in the four selected sites in the crystal nodules found in the cartilage of 12- and 20-week UAC groups.

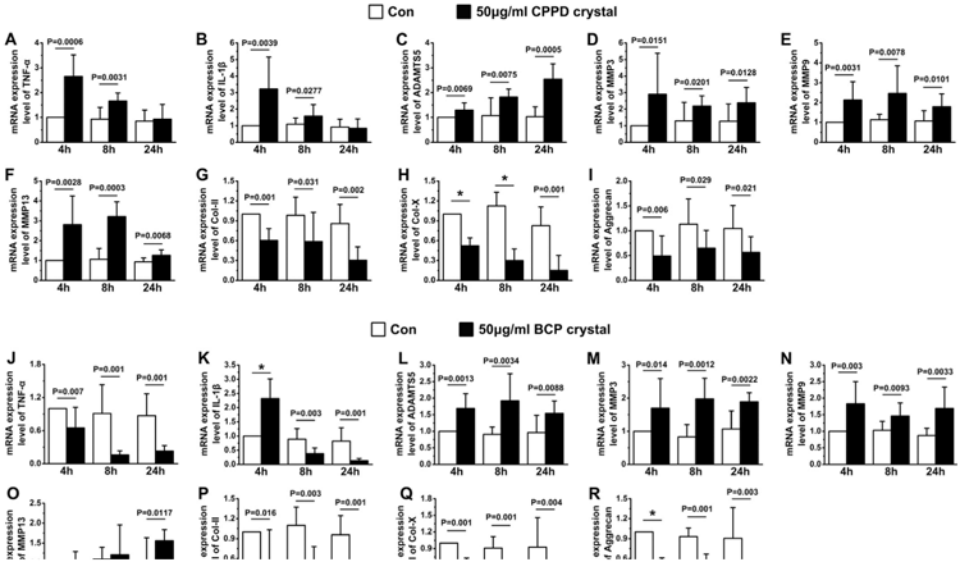

Fig. 7.

The effects of CPPD (AeI) and BCP (JeR) on the expression of *Tnf-α* (A, J), *Il-1β* (B, K), *Adamts5* (C, L), *Mmp3* (D, M), *Mmp9* (E, N), *Mmp13* (F, O), *Col-II* (G, P), *Col-X* (H, Q), and *Aggrecan* (I, R) RNA in cultures of chondrogenic ATDC5 cells after 4, 8, and 24 h of treatments. Values are represented as the mean with lower and upper limits of 95% CI. $n = 4$ separate cultures; $*P < 0.0001$ or as specified.

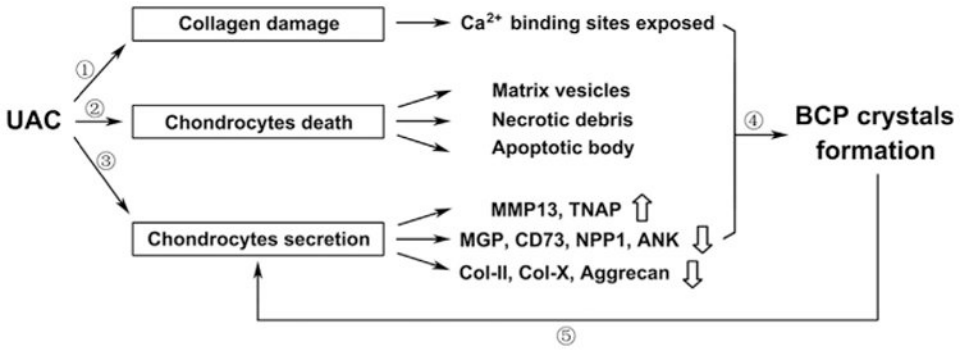

Fig. 8.

Schema for the effects of UAC on the BCP crystals formation in osteoarthritic cartilage. ①Abnormal mechanical force induced by UAC led the fragmentation of collagen fibers, making the Ca^{2+} binding site of the collagen fibers exposed. ② UAC stimulated cell death to produce matrix vesicles and apoptotic bodies to serve as mineral nucleation sites. ③UAC down-regulated the expression of inhibitors of mineralization accompanied with the up-regulation of TNAP and MMP13. ④The above changes contributed to the mineral deposition, especially BCP crystals. ⑤Mineral crystals served as a feed-forward signal to reduce production of matrix protein and enhanced the secretion of matrix degrading enzymes, thus further accelerating the cartilage degeneration.